Proving the contact rules for phase regions: Implications to phase diagrams of metal–hydrogen systems

V.E. Antonov [a,b,*], I.A. Sholin [a,c]

[a] *Institute of Solid State Physics RAS, 142432 Chernogolovka, Russia*
[b] *National University of Science and Technology 'MISIS', 119049 Moscow, Leninskii prosp. 4, Russia*
[c] *Moscow State University, Vorob'evy gory, Moscow 119992, Russia*

A B S T R A C T

The rule of triple joints has recently been proved for two-dimensional phase diagrams and two-dimensional sections of phase diagrams of a higher dimension (Antonov, 2013). The present paper is extending this rule to phase diagrams of binary metal–hydrogen systems composed of a metal immersed in a hydrogen gas. The rule is shown to be valid for every triple point in the temperature–pressure phase diagrams of these systems, including the points with the intersecting boundary lines tangent to each other. The paper also considers the sufficient conditions for the application of the rule to triple points in the projections of phase diagrams onto the temperature–concentration plane.

© 2015 Elsevier B.V. All rights reserved.

1. Introduction

The rules (or theorems) related to the topology of phase diagrams are very few. These include the Palatnik–Landau contact rule for phase regions [1] and two its consequences, the cross rule [1] and the Rhines phase rule [2], and also the rule of triple joints. The paper below will present the part of the talk concerning the rule of triple joints. This rule places limitations on the mutual position of three boundary lines meeting at one point in a two-dimensional phase diagram or in a two-dimensional section of a phase diagram of a higher dimension. The rule is usually formulated as follows:

The extension of the boundary line between two phase regions beyond the point of intersection with the boundaries of a third region should lie inside this third region.

The rule for triple joints is widely used in constructing equilibrium phase diagrams and in the error tests. However, for a very long time, the rule has only been proved for triple joints in the *T–P* diagrams of one-component systems [3]. The proof was based on the possibility to extend each of the three lines of phase equilibria into the metastable region beyond the point of their intersection. This condition, however, is never fulfilled for the triple points in phase diagrams of other types.

It was only recently that we noticed that the rule of triple joints should already be valid if two out of the three boundary lines can have a metastable extension beyond the point of their intersection. This finding allowed us to advance an improved formulation of the rule [4]:

Let it be a point of a joint of three boundary lines in a two-dimensional diagram of phase equilibria or in a two-dimensional section of a diagram. If at least two of these lines allow a metastable extension beyond the point of the joint, the extension of each of the three lines should lie in the phase region bounded by the two other lines.

The rule in this new form is illustrated by Fig. 1.

For the analysis of some phase equilibria, a more detailed formulation of the rule can be recommended:

Let it be a point of a joint of three boundary lines in a two-dimensional diagram of phase equilibria or in a two-dimensional section of a diagram. If the boundary between two phase regions can have a metastable extension beyond the point of intersection with the boundaries of the third phase region, this extension lies between the boundaries of the third region. If metastable extensions are possible for two boundaries, the extension of each of the three boundaries lies in the region between two other boundaries.

As one can see, the proved rule does not specify the types of the axes on which the diagram is built (pressure *P*, temperature *T*, volume *V*, concentrations *x*, electric field, etc.), or the number of components of the system, or the type or variance of the phase equilibria presented in the diagram. This makes the rule more flexible and applicable to the analysis of two-dimensional sections of phase diagrams of heterogeneous systems with any given number

* Corresponding author at: Institute of Solid State Physics RAS, 142432 Chernogolovka, Russia.
  E-mail address: antonov@issp.ac.ru (V.E. Antonov).

of components. On the other hand, applying the rule in the improved form requires a more rigorous understanding of the term "metastable extension" of a phase boundary compared to its commonly accepted meaning.

Another significant requirement is that the diagram should unambiguously represent phase compositions of the regions adjoining the triple joint. This requirement is always fulfilled for two-dimensional sections of the $T–P–x$ and $T–V–x$ diagrams of heterogeneous systems for which the Gibbs phase rule [5] is known to be valid, i.e., for the systems in which each phase contains all the components, the pressure is isotropic everywhere, and the effects due to interfaces between different phases and due to the external fields are negligible. Before applying the rule to a triple point in a diagram of other type, one have to make sure that the three phase regions only meet at this point and do not overlap.

Conditions and some aspects of the application of the rule to the diagrams of the Gibbs type were considered in Ref. [4]. This paper will consider a special case of phase diagrams of binary metal–hydrogen system, in which a metallic sample is brought in thermodynamical equilibrium with a H_2 gas surrounding it.

2. Temperature–pressure phase diagrams

There are basically two types of phase equilibria in the metal–hydrogen systems.

Many metals (rare earths, titanium, zirconium, etc.) easily absorb hydrogen at low pressures and do not lose it in inert media, even at elevated temperatures. The total hydrogen concentration in these metals can be varied independently of other parameters that also govern the phase state of the system (temperature, pressure, concentrations of different metallic components). Phase diagrams of the metal–hydrogen systems of this type have no specific features compared with the diagrams considered in Ref. [4].

Phase equilibria of another type are observed when a metal sample (one- or multicomponent) is immersed in an atmosphere of molecular hydrogen, and the temperature is high enough to establish the dynamical equilibrium between the hydrogen inside and outside the sample. In this case, the total concentration of hydrogen in the metal cannot be varied at will. Instead, the hydrogen concentration in each of the p_{cond} phases formed in the sample is determined by the equality $\mu_H^{(i)} = \frac{1}{2}\mu_{H_2}$, where $\mu_H^{(i)}(T,P)$ is the chemical potential of hydrogen in the i-th metallic phase ($i = 1, 2, \ldots, p_{cond}$) and $\mu_{H_2}(T,P)$ is the chemical potential of molecular hydrogen.

The line of the liquid–gas equilibrium in molecular hydrogen terminates at a critical point at $T_{cr} \approx 33$ K and $P_{cr} \approx 13$ bar [6] and the melting line of molecular hydrogen only rises to room temperature at $P \approx 5$ GPa and further to $T = 150\,°C$ at $P \approx 10$ GPa [7]. In

a wide $T–P$ range above the critical point and the melting line, molecular hydrogen behaves as a homogeneous gas (or fluid) and serves as pressure transmitting medium and a reservoir for loading the metal phase(s) with hydrogen up to the equilibrium concentrations, which vary with the temperature and pressure in a unique fashion.

Of special interest is the important case of systems composed of a one-component metal (or any other condensed substance, solid or liquid) reacting with H_2 gas taken in excess. The total number of phases in such a system with $n = 2$ components is $p = p_{cond} + 1$, and the Gibbs phase rule gives the variance (number of degrees of freedom)

$$f = n - p + 2 = 2 - (p_{cond} + 1) + 2 = 1 - p_{cond} + 2,$$

which looks exactly like that for the usual one-component system. Particularly, the maximum possible number of coexisting phases, p_{cond}, is three. This may occur if the number of degrees of freedom attains its minimum possible value, which is zero.

Correspondingly, the topology of the $T–P$ diagram describing phase states inside a one-component condensed substance surrounded with a hydrogen gas should be the same as that of a one-component system: equilibria between two condensed phases should be represented by curves, and three-phase equilibria by isolated points. The only difference is that the hydrogen concentration in each condensed phase varies with T and P.

By way of illustration, Fig. 2a shows a $T–P$ diagram of the Mn–H system characterized by a rather large variety of phase transformations in the studied range of hydrogen pressures and temperatures. At atmospheric pressure, there are four modifications of manganese: α-Mn and β-Mn with complex cubic lattices, fcc γ-Mn and bcc δ-Mn. The maximum hydrogen solubility in α-Mn and β-Mn is a few atomic percent [8]. The atomic ratio $x = H/Mn$ of solid hydrogen solutions in γ-Mn reaches $x = 0.36$ at $P = 0.8$ GPa and $T = 1000\,°C$ [8] and further increases to $x = 0.41$ at 2 GPa and $800\,°C$ [9] and to no less than $x = 0.72$ at 5 GPa and $900\,°C$ [10]. The hydrogen content of the ε hydride (hcp metal lattice) at $T = 350\,°C$ varies from $x \approx 0.8$ at 1 GPa to $x \approx 0.95$ at 4 GPa [8]. The composition of the ε′ hydrides (double hcp metal lattice) is expected to be similar to that of the ε hydrides and the hydrogen content of the Mn–H liquids is not known [10]. The interaction of high-pressure hydrogen with δ-Mn has not been studied. The boundary lines in Fig. 2a show the conditions of decomposition of the hydrides, and these conditions should be close to those of the corresponding phase equilibria (see [11] for discussion and explanation).

The significant differences and variations of hydrogen concentrations in the Mn–H phases have no impact on the applicability of the rule of triple joints to the $T–P$ diagram because the temperature and pressure are the same in these phases. Moreover, the rule must be valid for each triple point in the diagram, because every boundary line representing a two-phase equilibrium can be extended metastably (remains thermodynamically feasible) beyond the point of its intersection with the boundaries of the stability region of a third phase. This can be demonstrated in the same way as with the usual one-component systems [4].

Indeed, let us consider triple point 1 in Fig. 2a and imagine that the γ phase fails to form for some reasons (e.g., for kinetic ones). In the absence of this phase, both α and ε phases can exist in the γ region of the diagram and be in equilibrium with each other and this equilibrium will be represented by a metastable extension of the α/ε boundary. Similarly, the absence of the ε phase allows the extension of the α/γ boundary in the ε region, and the ε/γ boundary will have a metastable extension in the α region if the α phase does not form.
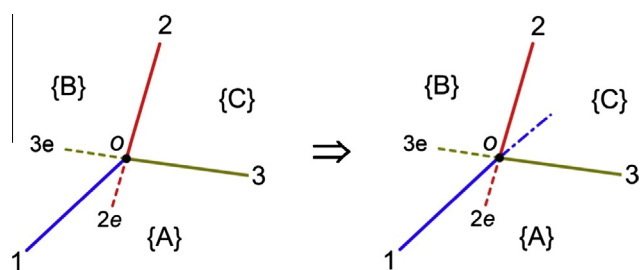

Fig. 1. Boundaries between phase regions (solid lines) and metastable extensions of these boundaries (dashed lines) near the point O of the triple joint. The dash-dotted line in the right-hand diagram represents a formal extension of boundary 3 predicted by the rule of triple joints. The phase states {A}, {B}, and {C} may differ in both the full number and the set of phases.
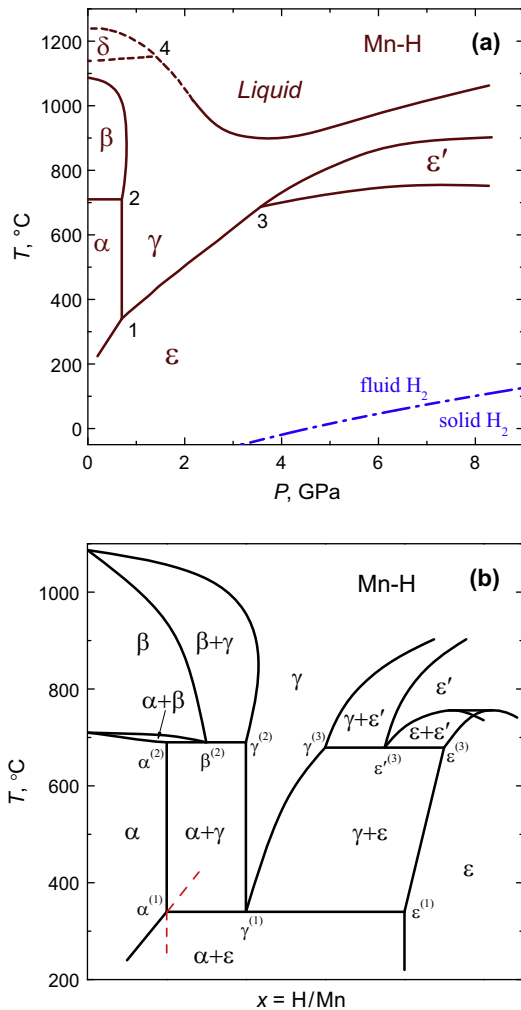
Fig. 2. (a) Experimental T–P phase diagram of the Mn–H system. The lines of the $\alpha \leftrightarrow \varepsilon$, $\alpha \leftrightarrow \gamma$, $\gamma \leftrightarrow \varepsilon$, $\alpha \leftrightarrow \beta$ and $\beta \leftrightarrow \gamma$ equilibria were determined in Ref. [8]. The lines of the $\varepsilon \leftrightarrow \varepsilon'$ and $\varepsilon' \leftrightarrow \gamma$ equilibria, the melting line of the γ phase and the hypothetical boundaries of the δ region are from Ref. [10]. The dash-dotted line at the bottom of the figure represents the melting line of molecular hydrogen [7]. (b) Tentative T–x projection of the T–P–x diagram of the Mn–H system. The symbols with upper indices mark the phases involved in invariant equilibria at the corresponding triple points in figure (a). Proportions along the H/Mn axis are skewed in order to better demonstrate the types of equilibria observed in narrow composition ranges. The equilibria with the liquid are not shown because of the unknown molar volume and hydrogen content of the Mn–H melts.

3. Clapeyron's equation

As can easily be shown, in the binary Me–H systems with excess hydrogen there is an analog of Clapeyron's equation derived for one-component systems. In the most general form, a two-phase equilibrium in the Me–H system can be written as $MeH_x + \frac{y-x}{2} H_2 = MeH_y$. Differentiating the corresponding equation $G_{MeH_x} + \frac{y-x}{2} G_{H_2} = G_{MeH_y}$ for the Gibbs energies along the line of equilibrium between the MeH_x and MeH_y phases in the T–P phase diagram and taking into account that $(\partial G/\partial P)_T = V$ and $(\partial G/\partial T)_P = -S$, we arrive at:

$$dT/dP = \Delta V/\Delta S, \tag{1}$$

where ΔV and ΔS are the total volume and entropy change of the system undergoing the above reaction.

If applied to the T–P diagram of the Mn–H system shown in Fig. 2a, this analog of the Clapeyron equation demonstrates, in

particular, that $\Delta V = 0$ for the phase transformations at the minimum of the melting line of the γ phase at ~ 3.5 GPa and 900 °C and at the shallow maximum of the $\varepsilon \leftrightarrow \varepsilon'$ equilibrium line at ~ 7 GPa and 750 °C, because $dT/dP = 0$ in both cases.

Results of the *in situ* X-ray measurements [10] allow estimating the maximum possible difference $\Delta V_{\varepsilon \to \varepsilon'} = |V_{\varepsilon'} - V_{\varepsilon}| \leqslant 0.1$ Å^3/atom Mn ≈ 0.06 cm^3/mol Mo between the volumes of the ε' and ε phases near the maximum of the $\varepsilon \leftrightarrow \varepsilon'$ line. In order that the total volume effect of the $\varepsilon \to \varepsilon'$ transition be zero, this transition should be accompanied by a change of $\Delta V_{gas} = -\Delta V_{\varepsilon \to \varepsilon'}$ in the volume of the molecular hydrogen surrounding the sample. The H$_2$ gas compressed to 7 GPa at 750 °C has $V_{gas} = 8.85$ cm^3/mol H$_2$ [12] therefore the difference between the hydrogen contents of the ε' and ε phases should not exceed $\Delta(H/Mn) = 2\Delta V_{\varepsilon \to \varepsilon'}/V_{gas} \leqslant 0.015$. Since the composition of the ε hydride is known to be close to MnH at a pressure of 7 GPa [8], using Eq. (1) thus predicts that the composition of the ε' hydride is close to MnH, too.

The usefulness of Eq. (1) for error tests of T–P phase diagrams can be illustrated via the analysis of volume effects accompanying the $\alpha \to \gamma$ transition in the Cr–H system studied earlier by *in situ* X-ray diffraction [13]. As seen from Fig. 3, the line of the $\alpha \to \gamma$ transition passes through a minimum at $P \approx 2.3$ GPa and $T \approx 755$ °C. Near this point, the dilute α solution of hydrogen in *bcc* chromium has $x_\alpha = H/Cr \approx 0.03$ and $V_\alpha \approx 12.23$ Å^3/atom Cr, while the γ phase with an *fcc* metal lattice has $V_\gamma \approx 15.05$ Å^3/atom Cr [13]. The authors of Ref. [13] assumed the γ phase to be a hydride with the composition close to CrH throughout the T–P range labeled "γ" in Fig. 3. However, from the condition $\Delta V_{\alpha \to \gamma} + \Delta V_{gas} = 0$ at the point of minimum and from $\Delta V_{\alpha \to \gamma} = V_\gamma - V_\alpha \approx 2.82$ Å^3/atom Cr = 1.70 cm^3/mol Cr and $V_{gas} = 13.87$ cm^3/mol H$_2$ [12] at this point it follows that the hydrogen content of the γ phase should be $x_\gamma = x_\alpha + 2\Delta V_{\alpha \to \gamma}/V_{gas} \approx 0.03 + 0.41 = 0.44$.

The most likely explanation of the resulting discrepancy is that the $\alpha \to \gamma$ line presented in Fig. 3 is not constructed correctly, because the γ phase with $V_\gamma \approx 15.05$ Å^3/atom Cr cannot have $x_\gamma = 0.44$ if it is composed of chromium and hydrogen. First, a chromium hydride with the *fcc* metal lattice and H/Cr ≈ 1 can be prepared by cathodic electrodeposition of chromium, and the atomic volume of such a hydride is 14.31 Å^3/atom Cr at $T = 8$ K and ambient pressure (see [14] and references therein). The existence of

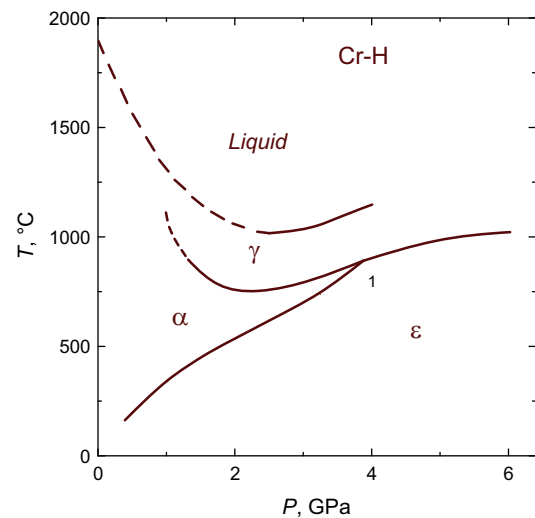**Fig. 3.** Experimental T–P phase diagram of the Cr–H system [13]. Phase α is a dilute solid hydrogen solution in *bcc* Cr; the ε phase is chromium hydride with the *hcp* metal lattice and composition close to CrH; the γ phase with the *fcc* metal lattice is also supposed to be a nearly stoichiometric hydride CrH; hydrogen concentrations in the γ phase and Cr–H liquids were never measured.

another *fcc* hydride, the γ phase, with a similar (and even larger) atomic volume and approximately two times less hydrogen content is very unlikely, because the high pressure would stabilize the denser phase. Second, hydrogenation of 3*d*-metals is known to increase their atomic volume at a rate varying from ≈ 2.0 Å^3/atom H for cobalt [15] to ≈ 3.0 Å^3/atom H for nickel [16]. Assuming that the increase $\Delta V_{\alpha \to \gamma}$ in the atomic volume of chromium is due to the absorption of $\Delta x = 2\Delta V_{\alpha \to \gamma}/V_{gas}$ of hydrogen suggests an incredibly high value of $\Delta V_{\alpha \to \gamma}/\Delta x = 2.82/0.41 \approx 6.9$ Å^3/atom H.

4. Additive relations and degenerate triple points in the temperature–pressure diagrams

In full analogy with usual one-component systems, one can also use the additive relations for the three changes in volume, ΔV_i, and three changes in entropy, ΔS_i, accompanying phase transitions around the triple point:

$$\Delta V_1 + \Delta V_2 + \Delta V_3 = 0 \text{ and } \Delta S_1 + \Delta S_2 + \Delta S_3 = 0 \quad (2)$$

Using Eqs. (1) and (2), it can be demonstrated that triple joints cannot appear as a smooth line crossed by another line at a finite angle, which is rather often found in experimental phase diagrams. As an example, Fig. 4a shows on a larger scale a vicinity of triple point 3 in the Mn–H system. The γ/ε and γ/ε′ boundary lines intersecting at this point make a common line without a break, and the ε/ε′ line crosses it.

Let us consider a triple joint shown in Fig. 4b, where lines 1 and 2 have equal slopes $(dT/dP)_1 = (dT/dP)_2$ at the point O of their intersection with line 3. Using Eq. (1) gives $\Delta V_1/\Delta S_1 = \Delta V_2/\Delta S_2$ at point O. Solving this equation together with Eq. (2) under the assumption that $\Delta S_3 \neq 0$ leads to $\Delta V_3/\Delta S_3 = \Delta V_1/\Delta S_1 = \Delta V_2/\Delta S_2$. Using Eq. (1) again, we get:

$$(dT/dP)_3 = (dT/dP)_1 = (dT/dP)_2. \quad (3)$$

This suggests that point O should be a tangency point of all three boundary lines.

Metastable extensions of lines 1, 2, and 3 can only intersect at point O and do not coincide with any of these stable lines or among
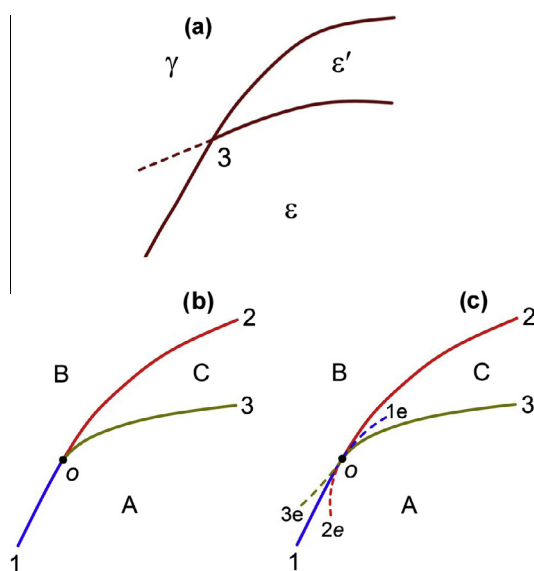
themselves. For example, if the extension of line 1 representing equilibrium between phases A and B had another common point with line 2 representing equilibrium between phases B and C, then this would be a second point of the three-phase equilibrium A + B + C. At the same time, the Gibbs phase rule only allows one such point. Similar considerations are also valid for the intersections of all other pairs of stable and metastable boundaries near point O. Since all these boundaries have one and only one common point O, the rule of triple joints is fully applicable to it. A possible arrangement of the metastable boundaries near the triple joint is shown in Fig. 4c.

In a special case of $\Delta S_3 = 0$ and $\Delta S_1 = -\Delta S_2 \neq 0$, solving the equation $(dT/dP)_1 = (dT/dP)_2$ together with Eqs. (1) and (2) gives $\Delta V_3 = 0$. The condition that both ΔS_3 and ΔV_3 are zero is fulfilled if line 3 terminates at a critical point coinciding with triple point O in the T–P diagram. If this happens, the value of $(dT/dP)_3$ at point O will be uncertain and line 3 will have no metastable extension beyond this point. We can, however, consider the situation with line 3 passing through point O, so that the critical point appears beyond it. Now, even if the critical point is infinitely close to point O, the three boundary lines must obey Eq. (3) and be tangent to each other at the point of intersection. Correspondingly, the joint will look like that in Fig. 4b irrespective of whether line 3 terminates at a critical point or not. Further, if lines 1 and 2 allow metastable extensions beyond point O, the extensions of all three lines will obey the rule of triple joints, though the extension of line 3 will not describe any phase equilibrium.

5. Projections of phase diagrams onto the temperature–concentration plane

If an independent axis of the overall hydrogen concentration in the metal is added to a T–P phase diagram of a binary Me–H system, the resultant T–P–x diagram will consist of curved surfaces located above the single-phase regions in the T–P diagram. These surfaces will be connected with each other by ruled two-phase surfaces perpendicular to the T–P plane and projecting onto the boundary lines in it. Most T–x and P–x sections of such a three-dimensional phase diagram are not very informative, and it is customary to present T–x and P–x projections of the curved and ruled surfaces constructed in a certain interval of, respectively, hydrogen pressures and temperatures. At low and moderate hydrogen pressures, the projections of different surfaces do not often overlap because the increase ΔV_{cond} in the volume of a metal sample due to the hydrogen absorption is much lower than the resulting decrease ΔV_{gas} in the volume of gaseous hydrogen.

In fact, consider the reaction $MeH_x + \frac{y-x}{2}H_2 = MeH_y$. At constant temperature, the pressure-induced gain in the Gibbs energy of this reaction is $\Delta G = \int_{P0}^{P} \Delta V dP$ and it is therefore fully determined by the negative volume effect of the reaction $\Delta V = (V_{MeH_y} - V_{MeH_x}) - \frac{y-x}{2}V_{H_2} = \Delta V_{cond} + \Delta V_{gas} < 0$.

As a result, the increase in the H_2 pressure leads to the increase in the hydrogen solubility in metallic phases and to the formation of new Me–H phases with a higher hydrogen concentration. This provides a one-to-one correspondence between the scales of pressure and concentration.

For example, no overlap of phase regions meeting at the triple points is observed in the T–x projection (Fig. 2b) of the T–P–x phase diagram of the Mn–H system. The rule of triple joints should therefore be valid for each of these points if not less than two of the three intersecting lines have metastable extensions.

Let us consider triple point $\alpha^{(1)}$ of the contact of phase regions $\{\alpha\}$, $\{\alpha + \varepsilon\}$ and $\{\alpha + \gamma\}$. Similar to what was said in Ref. [4] about triple points in the T–V diagrams of one-component systems, imagine that phase γ does not form. In this case, both α and ε phases

Fig. 4. (a) T–P diagram of the Mn–H system in the vicinity of triple point 3 (see Fig. 2a). The dashed line is an extension of the ε ↔ ε′ boundary beyond the triple point. (b and c) Triple point O of the adjacent T–P stability regions of phases A, B and C in the case of boundary lines 1 and 2 making a common line without a break. Stable boundaries 1, 2 and 3 are shown by the solid lines and metastable extensions 1e, 2e and 3e of these boundaries by the dashed lines.

can exist in the $\{\alpha + \gamma\}$ region, the boundary between regions $\{\alpha\}$ and $\{\alpha + \varepsilon\}$ can therefore be extended metastably beyond point $\alpha^{(1)}$ and, in accordance with the rule of triple joints (its more detailed version), this extension will be projected into region $\{\alpha + \gamma\}$ as shown by the dashed line in Fig. 2b. If the ε phase fails to form, then the boundary between regions $\{\alpha\}$ and $\{\alpha + \gamma\}$ can be extended beyond point $\alpha^{(1)}$ and the resulting line will reside in region $\{\alpha + \varepsilon\}$, which is also shown in Fig. 2b by a dashed line.

The boundary between regions $\{\alpha + \varepsilon\}$ and $\{\alpha + \gamma\}$ is formed by two superimposed tie-lines, $\alpha^{(1)}$–$\gamma^{(1)}$ and $\alpha^{(1)}$–$\varepsilon^{(1)}$. The position of points $\alpha^{(1)}$, $\gamma^{(1)}$, and $\varepsilon^{(1)}$ is uniquely determined by the conditions of the invariant equilibrium $\alpha + \gamma + \varepsilon$ and therefore the $\{\alpha + \varepsilon\}/\{\alpha + \gamma\}$ boundary cannot be extended metastably beyond point $\alpha^{(1)}$. Nevertheless, the formal extension of the $\{\alpha + \varepsilon\}/\{\alpha + \gamma\}$ boundary beyond point $\alpha^{(1)}$ should fall into region $\{\alpha\}$, in accordance with the rule of triple joints, since the existence of the metastable extensions for the other two boundaries meeting at point $\alpha^{(1)}$ ensures the fulfillment of this rule for all three boundaries. Analogous considerations lead to a conclusion on the validity of the rule of triple joints for all other five triple points in Fig. 2b as well (these are points labeled $\varepsilon^{(1)}$, $\alpha^{(2)}$, $\gamma^{(2)}$, $\gamma^{(3)}$, and $\varepsilon^{(3)}$).

It should be noted, however, that the increase in the hydrogen concentration in all Me–H phases with increasing pressure is not a sufficient condition for the absence of overlaps in the T–x projection of a T–P–x diagram. Particularly, there should be an interval of pressures with overlapping phase states around a point of maximum or minimum of the boundary curve in the T–P diagram (see the appearance of the $\{\varepsilon + \varepsilon'\}$ region in Fig. 2b).

Different phase regions will also overlap in the T–x projections of phase diagrams of the systems, in which hydrides have high-pressure modifications with the same H/Me ratio, but different crystal structures. The Mg–H system with MgH$_2$ dihydride experiencing a series of transformations at increasing pressure (see [17] and references therein) can serve as an example.

Besides, the one-to-one correspondence between the scales of pressure and hydrogen concentration in the condensed phases, which is usually observed at low and moderate pressures, can no longer hold true at higher pressures. This happens when a negative ΔV_{cond} of the transition to a phase with smaller hydrogen content can overweight the resulting positive ΔV_{gas}, rapidly decreasing with pressure due to the large compressibility of molecular hydrogen. The effect like this has already been observed in the binary H$_2$O–H$_2$ system, in which the sII phase (hydrogen clathrate hydrate) with a very loose crystal structure and the molecular ratio H$_2$/H$_2$O ~ 0.4 transforms at $P \approx 0.35$ GPa to the C$_0$ phase with a similar hydrogen content, and the C$_0$ phase further decomposes at $P \sim 0.8$ GPa to a mixture of the denser C$_1$ phase with a smaller ratio of H$_2$/H$_2$O ~ 0.1 and H$_2$ gas [18,19]. Because of the resulting overlaps of different phase regions in the T–x projection of the T–P–x phase diagram of the H$_2$O–H$_2$ system, some triple points in this projection do not obey the rule of triple joints, though the rule still remains applicable to every triple point in the T–P diagram.

6. Conclusions

Proving the rule of triple joints [4] allowed us to ascertain the sufficient conditions for its application to many types of phase diagrams of many different systems. The present paper considers phase diagrams of binary metal–hydrogen systems with the molecular hydrogen taken in excess. It is shown that as long as the hydrogen around the sample remains a homogeneous gas-like substance and undergoes no phase transitions, the T–P diagrams of such systems will look as networks of triple points connected with lines of two-phase equilibria, and the position of the lines near each point will obey the rule of triple joints. It is worth noting, too, that the rule will also be valid in the very large T–P range

below the melting curve of molecular H$_2$. The reason is that hydrogen does not experience any phase transitions in the solid state at pressures up to 300 GPa or even higher (see [7,20] and references therein). The crystalline hydrogen will therefore serve as homogeneous pressure transmitting medium and a reservoir for loading the metal samples with hydrogen up to the equilibrium concentrations, in full analogy with the gaseous hydrogen at lower pressures.

Regarding the domain of applicability of the rule and equations discussed in Sections 2–4, it seems also worth mentioning that the one-component metal (or other substance) does not necessarily consist of one chemical element. This can be a compound – say, LaNi$_5$ – and as long as the compositions of its hydrogenated phases can be written as LaNi$_5$H$_x$, the LaNi$_5$ "molecule" should be considered as a single component, and the LaNi$_5$–H system as a binary system.

Moreover, even non-stoichiometric alloys can interact with hydrogen as one-component substances, though the lines of their phase transformations can only be interpreted as metastable ones and the equilibrium phase states of the hydrogenated alloys may be quite dissimilar. For example, at high hydrogen pressures and temperatures above 250 °C, hydrides of disordered *fcc* Pd–Cu alloys form superstructures composed of alternating Cu and PdH layers [21,22] and hydrides of disordered *fcc* Pd–Ni alloys irreversibly decompose to a hydride of nearly pure Ni and a hydride of Pd with a few atomic per cent Ni [23]. Nevertheless, if two or more hydrogenated phases have the same composition of the metal sublattice, the equilibrium among them and the surrounding hydrogen gas should obey every rule for binary metal–hydrogen systems irrespective of whether the equilibrium is stable or metastable.

References

[1] L.S. Palatnik, A.I. Landau, Phase Equilibria in Multicomponent Systems, Holt, Rinehart and Winston, New York, 1964.
[2] F.N. Rhines, Phase Diagrams in Metallurgy, McGraw-Hill, New York, 1956.
[3] F.A.H. Schreinemakers, In-, mono- and divariant equilibria I, K. Ned. Akad. Wet. Proc. 18 (1) (1915) 116–126.
[4] V.E. Antonov, A rule for a joint of three boundary lines in phase diagrams, Phys. – Uspekhi 56 (4) (2013) 395–400.
[5] J.W. Gibbs, On the equilibrium of heterogeneous substances, Trans. Connect. Acad. 3 (1876) 108–248.
[6] The Air Liquide Gas Encyclopedia, <http://encyclopedia.airliquide.com/Encyclopedia.asp?GasID=36>.
[7] F. Datchi, P. Loubeyre, R. LeToullec, Extended and accurate determination of the melting curves of argon, helium, ice (H$_2$O), and hydrogen (H$_2$), Phys. Rev. B 61 (10) (2000) 6535–6546.
[8] V.E. Antonov, T.E. Antonova, N.A. Chirin, E.G. Ponyatovsky, M. Baier, F.E. Wagner, T–P phase diagram of the Mn–H system up to 4.4 GPa and temperatures to 1000 °C, Scr. Mater. 34 (8) (1996) 1331–1336.
[9] V.E. Antonov, K. Cornell, B. Dorner, V.K. Fedotov, G. Grosse, A.I. Kolesnikov, F.E. Wagner, H. Wipf, Neutron spectroscopy of γ manganese hydride, Solid State Commun. 113 (10) (2000) 569–572.
[10] Y. Fukai, T. Haraguchi, H. Shinomiya, K. Mori, Constitution of the Mn–H system at high hydrogen pressures, Scr. Mater. 46 (2002) 679–684.
[11] V.E. Antonov, A.I. Latynin, M. Tkacz, T–P phase diagrams and isotope effects in the Mo–H/D systems, J. Phys.: Condens. Matter 16 (46) (2004) 8387–8398.
[12] M. Tkacz, A. Litwiniuk, Useful equations of state of hydrogen and deuterium, J. Alloys Comp. 330–332 (2002) 89–92.
[13] Y. Fukai, M. Mizutani, Phase diagram and superabundant vacancy formation in Cr–H alloys, Mater. Trans. 43 (5) (2002) 1079–1084.
[14] V.E. Antonov, A.I. Beskrovnyy, V.K. Fedotov, A.S. Ivanov, S.S. Khasanov, A.I. Kolesnikov, M.K. Sakharov, I.L. Sashin, M. Tkacz, Crystal structure and lattice dynamics of chromium hydrides, J. Alloys Comp. 430 (2007) 22–28.
[15] V.K. Fedotov, V.E. Antonov, T.E. Antonova, E.L. Bokhenkov, B. Dorner, G. Grosse, F.E. Wagner, Atomic ordering in the hcp cobalt hydrides and deuterides, J. Alloys Comp. 291 (1999) 1–7.
[16] Y. Fukai, The Metal–Hydrogen System, Springer, Berlin, 1993.

[17] P. Vajeeston, P. Ravindran, B.C. Hauback, H. Fjellvåg, A. Kjekshus, S. Furuseth, M. Hanfland, Structural stability and pressure-induced phase transitions in MgH$_2$, Phys. Rev. B 73 (1) (2006) 224102.

[18] V.S. Efimchenko, M.A. Kuzovnikov, V.K. Fedotov, M.K. Sakharov, S.V. Simonov, M. Tkacz, New phase in the water–hydrogen system, J. Alloys Comp. 509S (2011) S860–S863.

[19] T.A. Strobel, M. Somayazulu, R.J. Hemley, Phase behavior of H$_2$ + H$_2$O at high pressures and low temperatures, J. Phys. Chem. C 115 (2011) 4898–4903.

[20] M.I. Eremets, I.A. Trojan, Evidence of maximum in the melting curve of hydrogen at megabar pressures, JETP Lett. 89 (4) (2009) 174–179.

[21] V.F. Degtyareva, V.E. Antonov, I.T. Belash, E.G. Ponyatovskii, Distortions of the F.C.C. crystal lattice of Pd$_{60}$Cu$_{40}$ alloy hydrogenated under high pressure, Phys. Stat. Sol. (a) 66 (1) (1981) 77–86.

[22] A.I. Kolesnikov, V.E. Antonov, A.M. Balagurov, S. Bennington, M. Prager, Neutron scattering studies of the structure and dynamics of the PdCu–H ordered phase produced under a high hydrogen pressure, J. Phys.: Condens. Matter 6 (43) (1994) 9001–9008.

[23] V.E. Antonov, T.E. Antonova, I.T. Belash, E.G. Ponyatovskii, V.I. Rashupkin, V.G. Thiessen, The Pd–Ni–H system at high pressure, Phys. Stat. Sol. (a) 77 (1) (1983) 71–79.